

## Research Article

# Analysis of Wellbore Stability considering the Interaction between Fluid and Shale

Long Chang <sup>1,2,3</sup> Haige Wang,<sup>1,2,3</sup> Lubin Zhuo,<sup>1,3</sup> Hongchun Huang,<sup>1,3</sup> Lingzhan Zou,<sup>1,3</sup> Qing Wang,<sup>1,2,3</sup> Hong Li,<sup>1,3</sup> and Jing Yu<sup>1,3</sup>

<sup>1</sup>CNPC Engineering Technology R&D Company Limited, Beijing, China

<sup>2</sup>PetroChina Research Institute of Exploration & Development, Beijing, China

<sup>3</sup>National Engineering Research Center of Oil & Gas Drilling and Completion Technology, Beijing, China

Correspondence should be addressed to Long Chang; changlongdri@cnpc.com.cn

Received 18 August 2022; Accepted 8 October 2022; Published 18 February 2023

Academic Editor: Peng Tan

Copyright © 2023 Long Chang et al. This is an open access article distributed under the Creative Commons Attribution License, which permits unrestricted use, distribution, and reproduction in any medium, provided the original work is properly cited.

Reservoir shale has the characteristics of bedding planes, strong anisotropy, and strong imbibition ability under ultralow water saturation, which has an important impact on wellbore stability of horizontal wells. Therefore, the physical and chemical properties of reservoir shale were analyzed, and a mechanics model of wellbore stability was established considering the elasticity and strength anisotropy. The wellbore stability was analyzed considering the anisotropy parameters of formation elasticity and strength and imbibition conditions. The results show that the anisotropy of elasticity and strength under the condition of imbibition are important parameters for evaluating the stability of reservoir shale borehole. Considering the interaction between fluid and reservoir shale, the weakening of the strength of the bedding structure is the reason for wellbore instability of reservoir shale. Bedding planes and microfractures provide rapid imbibition channel, and the imbibition volume increases, which further causes fracture expansion and strength weakening, and then leads to wellbore instability. Multistage effective plugging of bedding, microcracks and macroholes during drilling is the key to maintain the stability of shale wellbore.

## 1. Introduction

Horizontal well drilling and staged fracturing are the main technologies for the efficient development of shale oil and gas. Serious collapse of borehole wall during long horizontal drilling is the main technical difficulty, which seriously restricts the exploration and development process of shale oil and gas [1]. For the reservoir shale, the relevant scholars have established calculation models based on elastic anisotropy [2], weak plane failure criteria [3], quantitative characterization for the hydration cracks propagation of the hard and brittle shale [4], multifield coupling of the poroelasticity [5], etc., and then applied them to the analysis of wellbore stability of the shale oil and gas horizontal well.

Reservoir shale has the characteristics of bedding planes, strong anisotropy, and strong imbibition ability of the matrix and bedding fracture under ultralow water saturation. Under the low water saturation, water absorption pow-

ers of the reservoir shale matrix will be strengthened, and the water absorption powers mainly contain capillary force and chemical osmotic pressure [6]. Capillary force and chemical osmotic pressure determine the water absorption intensity per unit area of reservoir shale, while bedding planes and microcracks determine the water absorption area of reservoir shale matrix [7]. The bedding planes and micropores of reservoir shale can serve as the invasion channels of drilling fluid, which can intensify the evolution of meso-damages after shale hydration. In terms of macroscopic mechanical properties, the strength of shale decreases and the Young's modulus reduces, which is an important cause of borehole instability.

The conventional evaluation method of wellbore stability cannot correctly represent the wellbore stability of the reservoir shale. The wellbore stability was analyzed considering the interaction between fluid and shale, and it is necessary to introduce a new evaluation method.

## 2. Particularity of Reservoir Shale Wellbore Instability

*2.1. Conventional Evaluation Experiment for the Wellbore Stability.* Based on the drilling fluid technology of wellbore stability, the mud shale is divided into two categories by traditional classification methods: swelling mud shale and hard and brittle mud shale. Swelling mud shale contains montmorillonite clay minerals, with a strong hydration expansion and dispersion. The clay minerals of the hard and brittle mud shale are dominated by illite and illite/smectite mixed-layer, and the brittle shale rock developed rich bedding planes and microcracks.

Just like the swelling mud shale and hard and brittle mud shale, the gas shale has an ultralow matrix porosity and permeability. Shale reservoir is an extralow porosity and extralow permeability reservoir, which permeability is less than 10<sup>-3</sup> mD. The micro-nanopores develop well, the main pore diameter ranges from 80 nm to 200 nm, the specific surface area is large, and the structure is complex. Generally, the matrix porosity of shale is 2%-4%. In the shale gas reservoir, the content of various brittle minerals, such as quartz, feldspar, and carbonate, exceeds 40%, and the content of clay minerals is 25-40%, which mainly includes illite/smectite mixed-layer, illite, and chlorite. The wellbore stability of reservoir shale was evaluated by conventional method. The indoor evaluation test results of the shale fabric characteristics, physical and chemical properties, and wellbore stability are shown in Table 1.

The results of conventional comprehensive evaluation of the wellbore stability show that shale swelling of the Wufeng-Longmaxi formation in the reservoir interval is not strong, and the hydration dispersion ability is weak.

*2.2. Reservoir Shale Characteristics.* Marine shale in South China has a higher elastic modulus and lower Poisson's ratio, with a hard and brittle texture. Based on rock components, microstructure and hard and brittle mechanical characteristic, gas shale is usually classified as hard and brittle shale. Compared with the swelling shale and the hard and brittle shale, gas reservoir shale has special properties.

The rock mechanical characteristics of Wufeng-Longmaxi formation reservoir shale have the macroscopic and microscopic strength and elastic anisotropy. During the formation process of organic-rich shale, the crystalline particles of minerals, such as organic matter and clay mineral, are directionally arranged, and the elastic anisotropy of shale is caused by the bedding structure characteristics. The heterogeneity of reservoir shale is strong, and the bedding and microcracks are developed well. The widths of microcracks are generally between hundreds of nanometers and micrometers (Figure 1). On the macrolevel, shale bedding and microcrack have weak mechanical properties. Thus, reservoir shale has strength anisotropy.

Wufeng-Longmaxi formation reservoir shale has ultralow water saturation, and the initial water saturation is mainly in the range of 30%-50% (Figure 2), which is less than the maximum of the water saturation of bound water (70%). Ultralow water saturation of reservoir shale is mainly

TABLE 1: Conventional evaluation on the wellbore stability of reservoir shale.

Evaluation indicator	Results
Content of the illite/smectite mixed-layer mineral	14%, 10% (%S)
Zeta potential	-8 ~ -4 mV
Cation exchange capacity	<10 mmol/100 g
Specific surface area	14~23 m <sup>2</sup> /g
Roller recovery	>98%
Slope of capillary suction-time curve	0.0645
Linear expansion ratio	8-12%

caused by the hydrocarbon generation and drainage, as well as the vaporization and liquid carrying [8-10]. The water absorption powers of the reservoir shale matrix mainly contain two aspects: capillary force and chemical osmotic pressure. Under the low water saturation, both the two water absorption powers of the reservoir shale matrix will be strengthened.

The anisotropy reservoir shale bedding develops well, and the seepage capacity is directional. The shale imbibition experiments in parallel and vertical bedding directions were conducted. The spontaneous imbibition experiments were carried out on high precision electronic balances (model Mettler Toledo LE204E) with mass resolution of up to 0.0001 g. The rock samples were tied by a thin nylon filament attached to a metal bracket, and the metal bracket was settled on the mass sensor. The samples were fully submerged into beakers filled with deionized water, and the change in mass of the samples during the imbibition process was then transmitted to the mass sensor through the metal bracket. The mass data were logged by a computer once per minute. The four sides of the direction of the parallel bedding plane of the massive reservoir rock core are sealed, and the fluid enters along the vertical bedding direction during the imbibition process. In the same way, after sealing the two sides of the direction of the vertical bedding of rock core in the same layer, the fluid enters along the parallel bedding planes. The results of imbibition experiment of the reservoir shale are shown in Figure 3. The vertical ordinate is the normalization of imbibition quality to imbibition area, and the horizontal ordinate is the normalization of time.

According to the spontaneous imbibition curve of reservoir shale, compared with vertical bedding, the imbibition volume along the bedding direction is larger, and the imbibition rate is faster. The bedding provides a channel for rapid seepage, opens up more imbibition spaces, and promotes the total amount of imbibition and also increases the ratio of imbibition.

After the reservoir shale imbibes the fluid, the mechanical characteristics change of hydration is obvious, and microscopically, it promotes the generation, propagation, and connection of secondary microcracks. In terms of macroscopic mechanical properties, the strength of shale decreases, and the Young's modulus reduces [11] (Figure 4).

When researching the wellbore stability of reservoir shale, the above special properties of the shale should be

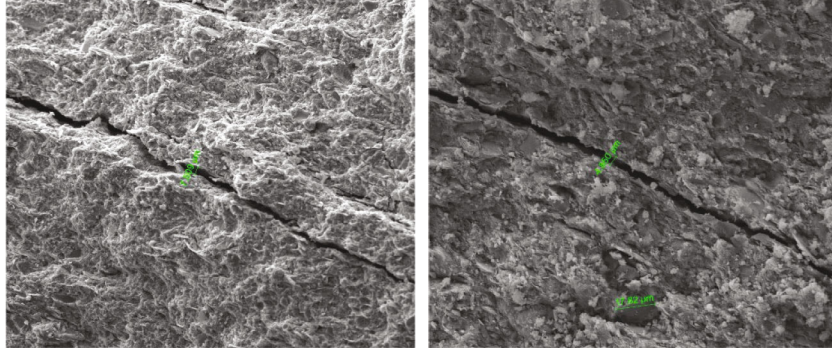


FIGURE 1: Characteristics of microbedding fractures in reservoir shale.

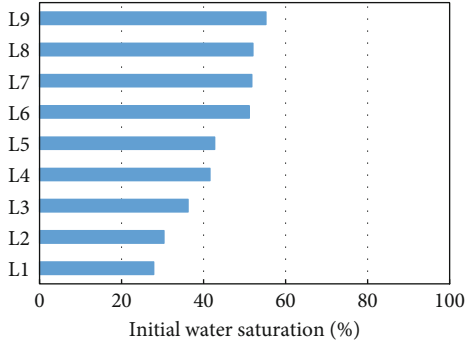


FIGURE 2: Initial water saturation of reservoir shale.

considered. In this paper, a mechanical model of wellbore stability considering the elasticity and strength anisotropy will be established, to analyze the mechanical response of shale water absorption in bedding, and then to make the analysis of wellbore stability considering the interaction between fluid and shale.

### 3. Mechanical Model of Shale Reservoir Wellbore Stability

**3.1. Stress Distribution at the Borehole Wall in Transverse Isotropic Formations.** Based on the complex function solution of generalized plane strain elasticity problem, circular-hole boundary conditions of stress distribution, the analytical expressions for the stress field are formulated [12–14]:

$$\begin{cases} \sigma_x = \sigma_{x,o} + 2 \operatorname{Re} \left[ \mu_1^2 \Phi_1'(z_1) + \mu_2^2 \Phi_2'(z_2) + \mu_3^2 \lambda_3 \Phi_3'(z_3) \right], \\ \sigma_y = \sigma_{y,o} + 2 \operatorname{Re} \left[ \Phi_1'(z_1) + \Phi_2'(z_2) + \lambda_3 \Phi_3'(z_3) \right], \\ \sigma_z = \sigma_{z,o} - \frac{1}{a_{33}} (a_{31} \sigma_{x,h} + a_{32} \sigma_{y,h} + a_{34} \tau_{yz,h} + a_{35} \tau_{zx,h} + a_{36} \tau_{xy,h}), \\ \tau_{xy} = \tau_{xy,o} - 2 \operatorname{Re} \left[ \mu_1 \Phi_1'(z_1) + \mu_2 \Phi_2'(z_2) + \mu_3 \lambda_3 \Phi_3'(z_3) \right], \\ \tau_{yz} = \tau_{yz,o} - 2 \operatorname{Re} \left[ \lambda_1 \Phi_1'(z_1) + \lambda_2 \Phi_2'(z_2) + \Phi_3'(z_3) \right], \\ \tau_{zx} = \tau_{zx,o} + 2 \operatorname{Re} \left[ \mu_1 \lambda_1 \Phi_1'(z_1) + \mu_2 \lambda_2 \Phi_2'(z_2) + \mu_3 \Phi_3'(z_3) \right], \end{cases} \quad (1)$$

where the derivatives of the analytic function  $\Phi_k(z_k)$  with respect to the variable  $z_k$  are given by

$$\begin{cases} \Phi_1'(z_1) = \frac{1}{2\Delta(\mu_1 \cos \theta - \sin \theta)} \left[ D'(\lambda_2 \lambda_3 - 1) + E'(\mu_2 - \lambda_2 \lambda_3 \mu_3) + F'(\mu_3 - \mu_2) \lambda_3 \right], \\ \Phi_2'(z_2) = \frac{1}{2\Delta(\mu_2 \cos \theta - \sin \theta)} \left[ D'(1 - \lambda_1 \lambda_3) + E'(\lambda_1 \lambda_3 \mu_3 - \mu_1) + F'(\mu_1 - \mu_3) \lambda_3 \right], \\ \Phi_3'(z_3) = \frac{1}{2\Delta(\mu_3 \cos \theta - \sin \theta)} \left[ D'(\lambda_1 - \lambda_2) + E'(\lambda_2 \mu_1 - \lambda_1 \mu_2) + F'(\mu_2 - \mu_1) \right]. \end{cases} \quad (2)$$

$\mu_k$  are the roots of the characteristic equation as

$$f(\mu) = l_4(\mu)l_2(\mu) - l_3^2(\mu) = 0, \quad (3)$$

where

$$\begin{cases} l_2(\mu) = \beta_{55}\mu^2 - 2\beta_{45}\mu + \beta_{44}, \\ l_3(\mu) = \beta_{15}\mu^3 - (\beta_{14} + \beta_{56})\mu^2 + (\beta_{25} + \beta_{46})\mu - \beta_{24}, \\ l_4(\mu) = \beta_{11}\mu^4 - 2\beta_{16}\mu^3 + (2\beta_{12} + \beta_{66})\mu^2 - 2\beta_{26}\mu + \beta_{22}. \end{cases} \quad (4)$$

$\beta_{ij}$  are the reduced strain coefficients and are defined as

$$\beta_{ij} = a_{ij} - \frac{a_{i3}a_{j3}}{a_{33}} \quad (i, j = 1, 2, 4, 5, 6). \quad (5)$$

Three complex numbers  $\lambda_k$  equal to

$$\lambda_1 = -\frac{l_3(\mu_1)}{l_2(\mu_1)}; \quad \lambda_2 = -\frac{l_3(\mu_2)}{l_2(\mu_2)}; \quad \lambda_3 = \frac{l_3(\mu_3)}{l_4(\mu_3)}. \quad (6)$$

The expressions of  $D'$ ,  $E'$ ,  $F'$ , and  $\Delta$  are

$$\begin{cases} D' = (P_w - \sigma_{x,o}) \cos \theta - \tau_{xy,o} \sin \theta - i[(P_w - \sigma_{x,o}) \sin \theta + \tau_{xy,o} \cos \theta], \\ E' = -(P_w - \sigma_{y,o}) \sin \theta + \tau_{yx,o} \cos \theta - i[(P_w - \sigma_{y,o}) \cos \theta + \tau_{yx,o} \sin \theta], \\ F' = -\tau_{zx,o} \cos \theta - \tau_{zy,o} \sin \theta - i[\tau_{zy,o} \cos \theta - \tau_{zx,o} \sin \theta], \\ \Delta = \mu_2 - \mu_1 + \lambda_2 \lambda_3 (\mu_1 - \mu_3) + \lambda_1 \lambda_3 (\mu_3 - \mu_2), \end{cases} \quad (7)$$

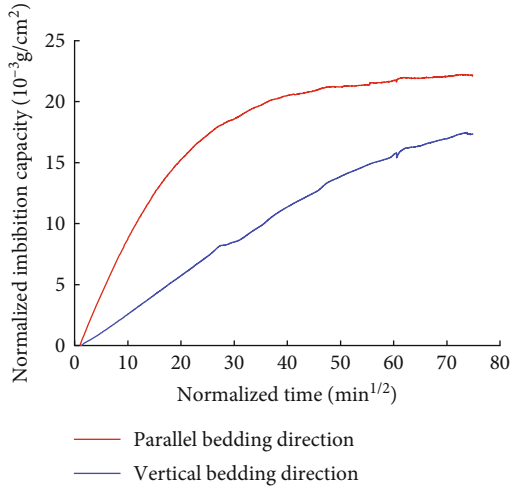


FIGURE 3: Spontaneous imbibition character of reservoir shale.

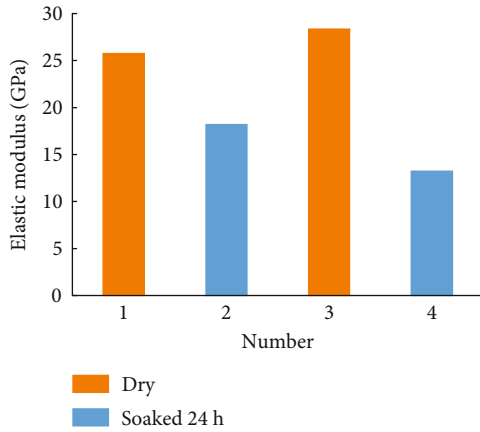


FIGURE 4: Changes in elastic modulus before and after soaked in water [11].

where  $\theta$  is the angle measured counter-clock wise from the  $\sigma_{x,o}$  axis.  $\sigma_{x,o}$ ,  $\sigma_{y,o}$ , and  $\sigma_{z,o}$  are the in situ normal stresses in  $x$ ,  $y$ , and  $z$  directions, respectively.  $\tau_{xy,o}$ ,  $\tau_{yz,o}$ , and  $\tau_{zx,o}$  are the in situ shear stresses in  $xy$ ,  $yz$ , and  $zx$  plane, respectively.  $P_w$  is the wellbore internal hydraulic pressure.

For transversely isotropic materials, the  $z$ -axis is taken to be consistent with the elasticity symmetry axis, and the flexibility coefficient is

$$\begin{cases} a_{11} = a_{22} = \frac{1}{E}; & a_{12} = -\frac{\nu}{E}; & a_{13} = a_{23} = -\frac{\nu'}{E'}, \\ a_{33} = \frac{1}{E'}; & a_{44} = a_{55} = \frac{1}{G'}; & a_{66} = \frac{1}{G} = \frac{2(1+\nu)}{E}, \end{cases} \quad (8)$$

where  $E$  and  $\nu$  are the elastic modulus and the Poisson's ratio in the isotropic plane, respectively.  $E'$  and  $\nu'$  are the elastic modulus and the Poisson's ratio in the normal direction of the isotropic plane, respectively.  $G'$  is the shear modulus of the plane which is vertical to the isotropic plane.

The flexibility coefficient in Equation (8) is the material characteristic of isotropic plane in the horizontal. The formation bedding plane inclines, and the constitutive equation needs to establish a relationship with the formation dip angle and formation dip direction. The wellbore stress solution is carried out in the well axis coordinate system, which needs to establish a relationship with the inclination angle and azimuth angle, requiring the coordinate transformation of the elastic constant.

### 3.2. Coordinate Transformation

**3.2.1. Coordinate Transformation of the Elastic Parameter.** The flexibility coefficient matrix  $A$  under the elastic main axis measured in the laboratory is transformed into the well axis coordinate system in two steps. The first step is the transformation between the formation media coordinate system and geodetic coordinate system (Figure 5(a)), and the transformation parameters are formation dip angle  $\beta$  and formation dip direction  $\alpha$ . The second step is the transformation between the geodetic coordinate system and well axis coordinate system (Figure 5(b)), and the transformation parameters are inclination azimuth angle  $\delta$  and inclination angle  $\gamma$ .

Calculation of coordinate transformation of the anisotropy elastic parameter:

$$[A''] = [Q][P][A][P]^T[Q]^T, \quad (9)$$

where  $A''$  is the flexibility coefficient matrix of the borehole coordinate system,  $A$  is the flexibility coefficient matrix of the formation media coordinate system, and  $P$  and  $Q$  are the transformation matrixes, respectively [15].

Substitute the transformed flexibility coefficient matrix into Equations (5), (3), and (6) to solve the relevant parameters, and then solve Expressions (2) and (1), respectively, to get transversely isotropic stratum wellbore stress.

**3.2.2. Coordinate Transformation of In Situ Stress.** In the wellbore stress analytic Expression (1), in situ stress is the stress component at any direction in the borehole coordinate system, and it needs to transform the three-dimensional in situ stress into the inclined shaft coordinate system with the wellbore parameter.

In situ stress coordinate transformation equation:

$$\begin{cases} \sigma_{x,o} = (\sigma_H \cos^2\varphi + \sigma_h \sin^2\varphi) \cos^2\gamma + \sigma_v \sin^2\gamma, \\ \sigma_{y,o} = \sigma_H \sin^2\varphi + \sigma_h \cos^2\varphi, \\ \sigma_{z,o} = (\sigma_H \cos^2\varphi + \sigma_h \sin^2\varphi) \sin^2\gamma + \sigma_v \cos^2\gamma, \\ \tau_{xy,o} = \frac{1}{2}(\sigma_h - \sigma_H) \sin 2\varphi \cos \gamma, \\ \tau_{xz,o} = \frac{1}{2}(\sigma_H \cos^2\varphi + \sigma_h \sin^2\varphi - \sigma_v) \sin 2\gamma, \\ \tau_{yz,o} = \frac{1}{2}(\sigma_h - \sigma_H) \sin 2\varphi \sin \gamma, \end{cases} \quad (10)$$

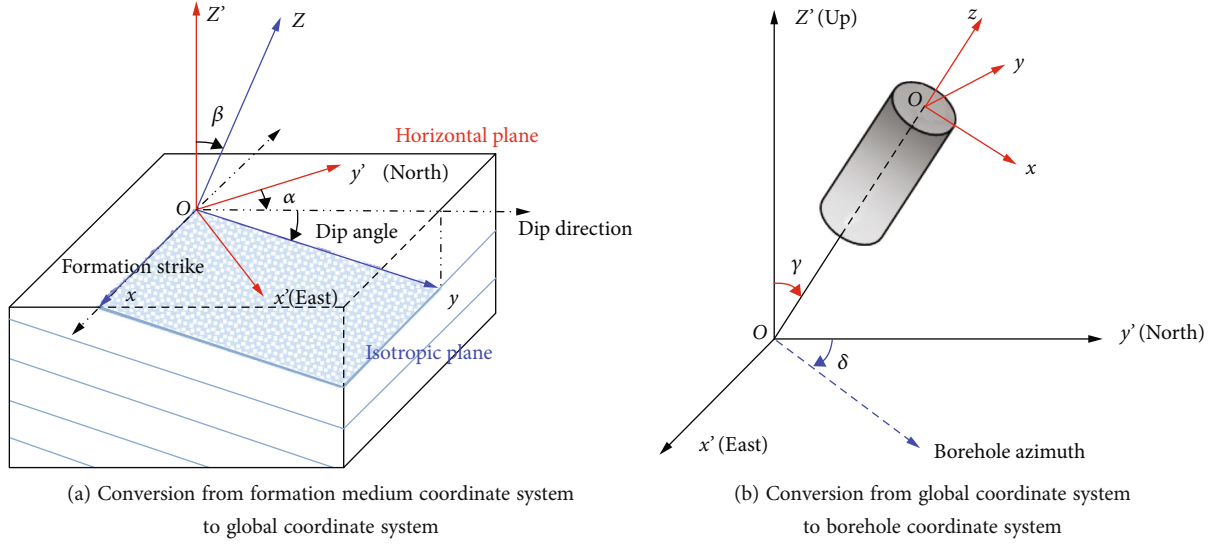


FIGURE 5: Coordinate transformation of the elastic constant.

where  $\sigma_H$  is the horizontal maximum in situ stress,  $\sigma_h$  is the horizontal minimum in situ stress, and  $\sigma_v$  is the vertical stress.  $\varphi$  is the azimuth angle of inclined borehole (that is, the included angle between the direction of deflection and horizontal maximum in situ stress direction) [16], and  $\gamma$  is the inclination angle.

**3.3. Strength Failure Criteria of Bedding Shale.** Considering the strength effect of shale bedding, the reservoir shale bedding develops, and the mechanical analysis of wellbore instability consists of two failure modes of anisotropic shale: intact rock and the weak plane.

**3.3.1. Failure Criterion of Intact Rock.** Al-Ajmi and Zimmerman [17] proposed Mogi-Coulomb criterion considering intermediate principal stress. The criterion can be written as

$$\tau_{oct} = \frac{2\sqrt{2}}{3} S_{oi} \cos \phi_i + \frac{2\sqrt{2}}{3} \sigma_m \sin \phi_i, \quad (11)$$

where  $\tau_{oct}$  is the octahedral shear stress,  $\tau_{oct} = 1/3 \sqrt{(\sigma_1 - \sigma_2)^2 + (\sigma_2 - \sigma_3)^2 + (\sigma_3 - \sigma_1)^2}$ .  $S_{oi}$  is the cohesion of intact rock, and  $\phi_i$  is the internal friction angle of intact rock.  $\sigma_m = 1/2(\sigma_1 + \sigma_3)$ ,  $\sigma_1$ ,  $\sigma_2$ , and  $\sigma_3$  are three principal stresses that can be calculated by solving the eigenvalues of stress tensor matrix in cylindrical coordinate systems or borehole coordinate system.

**3.3.2. Failure Criterion of Weak Plane.** The Mohr-Coulomb failure criterion for the weak plane is expressed by

$$\tau_w = S_{ow} \cos \phi_w + \sigma_w \sin \phi_w, \quad (12)$$

where  $\tau_w$  is the resultant shear stress on the weak plane,  $\tau_w = \sqrt{(\tau_{zx}^w)^2 + (\tau_{zy}^w)^2}$ .  $S_{ow}$  is the cohesion of weak plane, and  $\phi_w$  is the internal friction angle of weak plane.  $\sigma_w$  is

the normal stress on weak plane,  $\sigma_w = \sigma_z^w \cdot \sigma_z^w + \tau_{zx}^w$ , and  $\tau_{zy}^w$  are the stress component of stress tensor matrix in weak plane coordinate systems.

## 4. Analysis of Wellbore Stability of Bedding Shale

The horizontal well parameter, stratum mechanical parameter, and crustal stress parameter in the pilot test well area of Jiaoshiba in the Fuling shale gas field are comprehensively sorted out [18], as shown in Table 2, and some parameters in the table are reasonably assumed based on the related references. Substitute the calculation parameters into the mechanical model of shale reservoir wellbore stability in Section 3, control the variables appropriately, and analyze the influencing factors.

In situ stress is the most fundamental and important factor that influences the instability of reservoir shale wellbore. The magnitude of in situ stress, the difference of horizontal in situ stress, and the orientation of crustal stress all have an important impact on the stress distribution at the borehole wall in the anisotropy formation, and the equivalent density of safe drilling fluid. When the difference between the two horizontal in situ stresses increases, the stress difference in different parts of the inclined wellbore wall increases, and the angle of stress distribution around the borehole will also deflect. In the design of drilling fluid density, the determination of borehole wall failure pressure and failure position needs comprehensive consideration of in situ stress, horizontal in situ stress ratio, and in situ stress orientation. The in situ stress distribution in the study area is stable, and the horizontal wells are designed to be drilled along the direction of the minimum horizontal in situ stress. In this paper, it will not analyze the factor that influences the wellbore stability in terms of the magnitude and orientation of the in situ stress, but it is still emphasized that in situ stress has the most important effect on the wellbore stability

TABLE 2: Calculation parameters.

Type	Variables	Value	Unit
Well parameters	Vertical depth TVD	2380	m
	Inclination angle $\gamma$	90	$^{\circ}$
	Inclination azimuth angle $\delta$	0	$^{\circ}$
Formation parameters	Elastic modulus in the isotropic plane $E$	32.75	GPa
	Poisson's ratio in the isotropic plane $\nu$	0.14	—
	Elastic modulus of normal direction in the isotropic plane $E'$	27.02	GPa
	Poisson's ratio of normal direction in the isotropic plane $\nu'$	0.21	—
	Shear modulus of normal direction in the isotropic plane $G'$	13.14	GPa
	Formation dip direction $\alpha$	0	$^{\circ}$
	Formation dip angle $\beta$	30	$^{\circ}$
	Cohesive force of intact rock $S_{oi}$	45	MPa
	Internal friction angle of intact rock $\phi_i$	30	$^{\circ}$
	Cohesive force of weak plane $S_{ow}$	25	MPa
Internal friction angle of weak plane $\phi_w$	20	$^{\circ}$	
In situ stress parameters	Horizontal maximum in situ stress $\sigma_H$	63.50	MPa
	Horizontal minimum in situ stress $\sigma_h$	47.39	MPa
	Overlying crustal stress $\sigma_v$	58.62	MPa
	Horizontal maximum in situ stress orientation $\psi$	90	$^{\circ}$

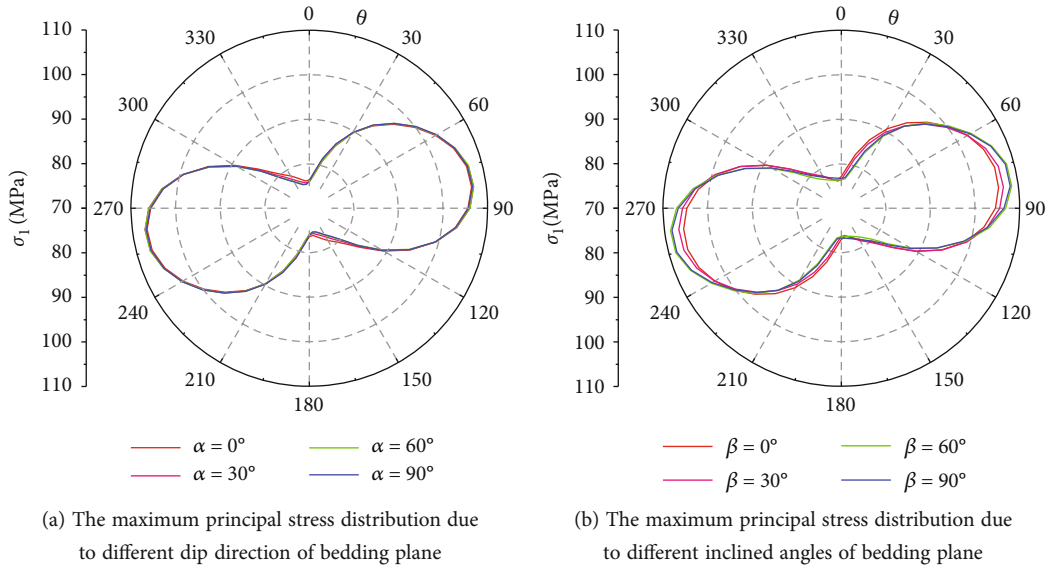
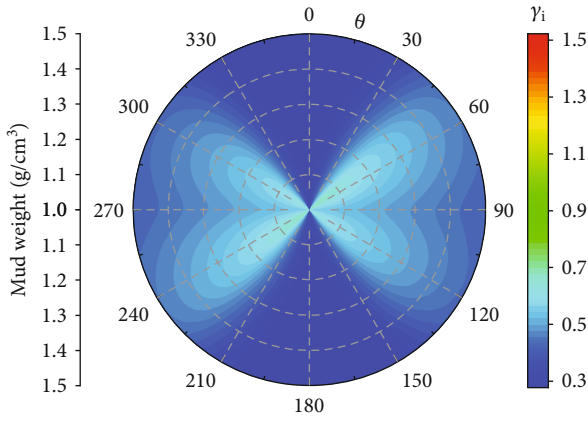


FIGURE 6: Influence of the inclined property of bedding plane on the principal stress at the borehole wall.

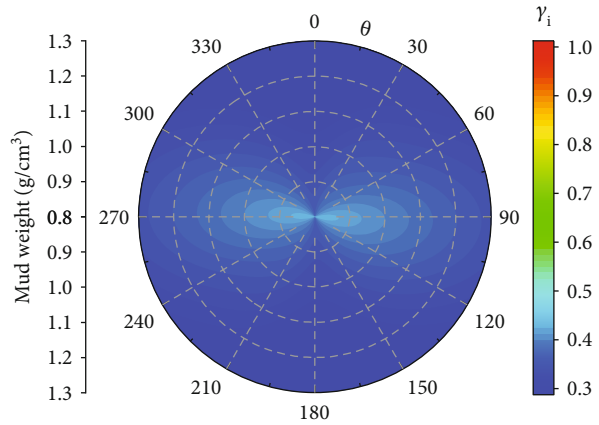
of bedding shale. Considering the bedding characteristics of gas shale reservoirs, this paper focuses on the analysis of the inclined stratum property and strength property of the bedding plane.

*4.1. Influence of the Inclined Property of Bedding Plane on the Principal Stress at the Borehole Wall.* A variable analysis was carried out on the influence of the inclined parameters of

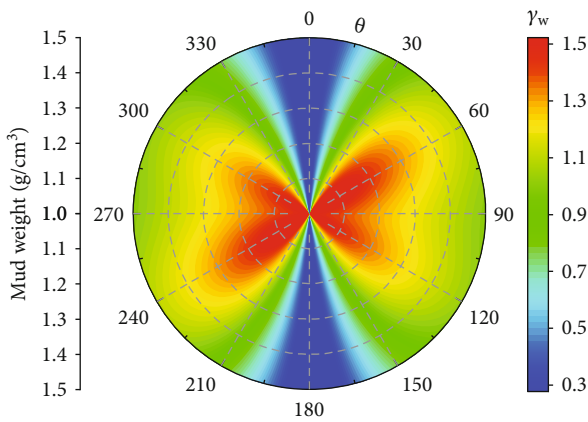
bedding plane under anisotropy. Keeping the well parameters, in situ stress parameters and formation elastic anisotropy parameters unchanged, the formation dip direction was taken as  $0^\circ$ ,  $30^\circ$ ,  $60^\circ$ , and  $90^\circ$  in turn to calculate the distribution of the maximum principal stress of wellbore around the well and plot it in polar coordinate system, as shown in Figure 6(a). In the same way, the variable analysis of the formation dip angle was also carried out, and the



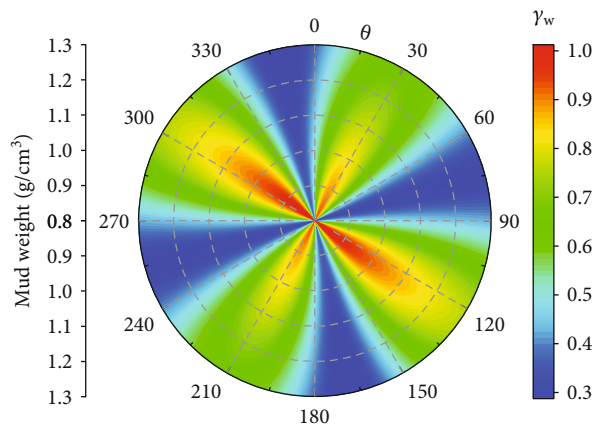
(a) The critical regions distribution due to different mud weight of intact rock with  $\beta = 30^\circ$  and  $\delta = 0^\circ$



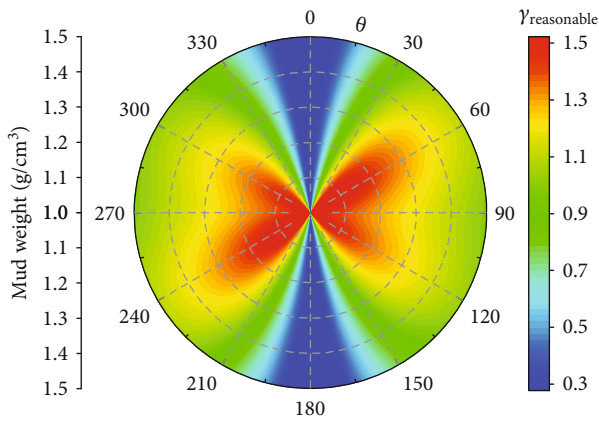
(b) The critical regions distribution due to different mud weight of intact rock with  $\beta = 20^\circ$  and  $\delta = 45^\circ$



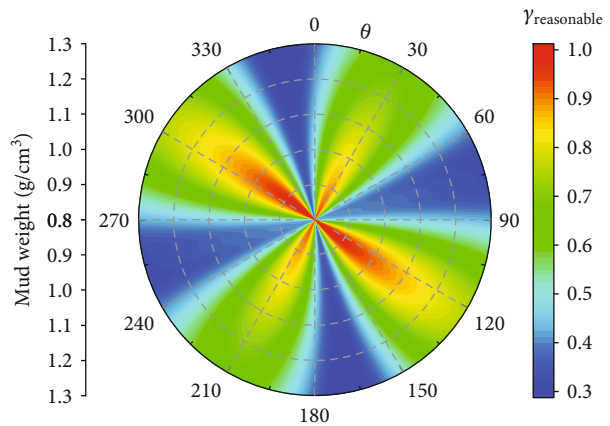
(c) The critical regions' distribution due to different mud weight of weak plane with  $\beta = 30^\circ$  and  $\delta = 0^\circ$



(d) The critical regions' distribution due to different mud weight of weak plane with  $\beta = 20^\circ$  and  $\delta = 45^\circ$



(e) The critical regions' distribution due to different mud weight with  $\beta = 30^\circ$  and  $\delta = 0^\circ$



(f) The critical regions' distribution due to different mud weight with  $\beta = 20^\circ$  and  $\delta = 45^\circ$

FIGURE 7: Borehole stability analysis of reservoir shale with considering weak plane.

maximum principal stress distribution of the wellbore in different inclined angles of bedding plane was shown in Figure 6(b).

Under the condition of anisotropy shale reservoirs, the inclination parameters of the bedding formation—the dip direction and dip angle—change equally from  $0^\circ$  to  $90^\circ$ ,

respectively. The distribution of the maximum principal stress at the borehole wall is not very different at each position around the well, and the position angle of the extremum of the maximum principal stress on the wellbore around the well is also the same. During the mechanical analysis of wellbore stability of anisotropy reservoir shale, the effect of

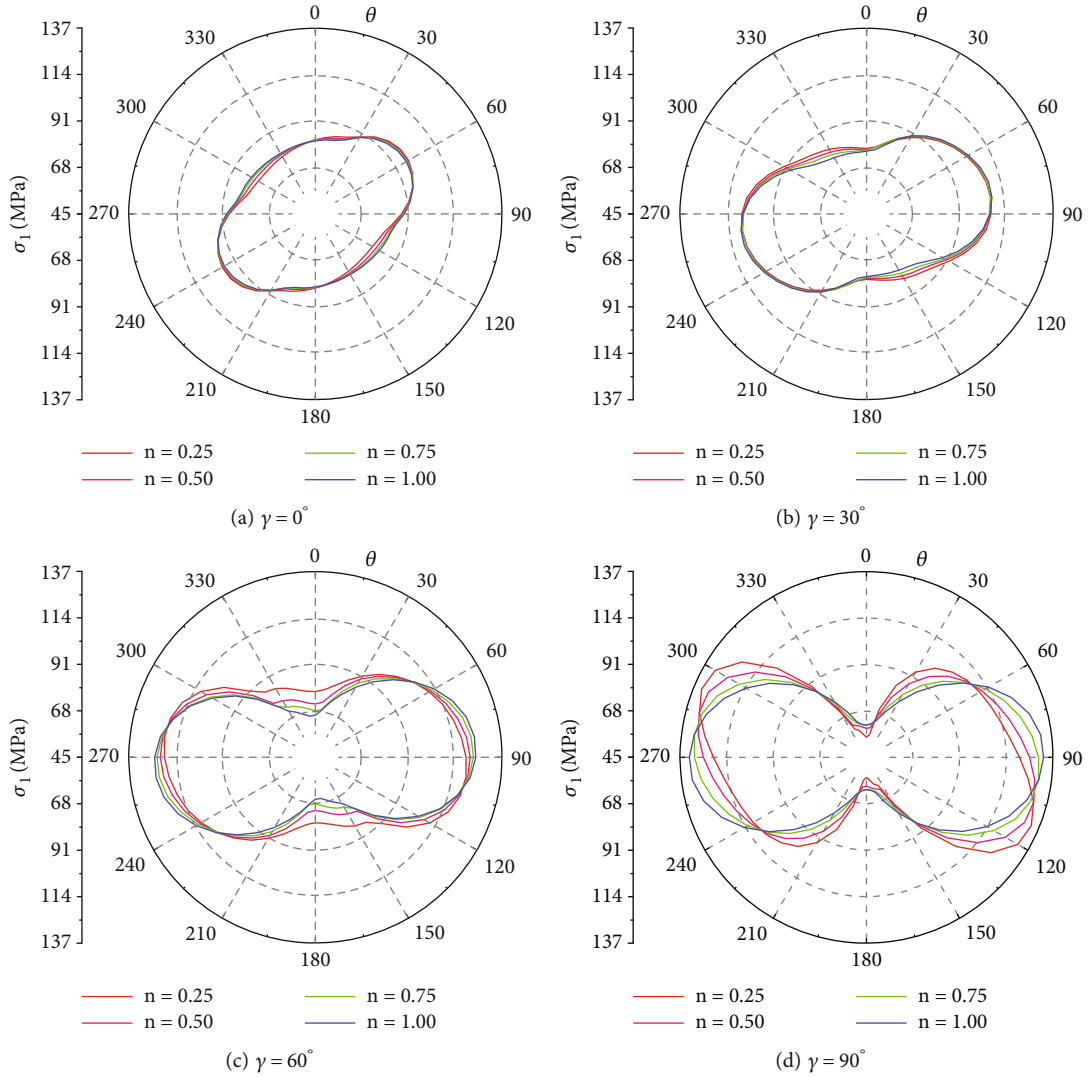


FIGURE 8: The maximum principal stress distribution due to different ratios of elastic modulus.

wellbore stress along with the dip direction and dip angle of bedding plane can be ignored.

**4.2. Influence of Strength Property of the Bedding Plane on the Wellbore Stability.** Using the method of Gao et al. [19], according to the Expressions (11) and (12) of the strength failure criteria of intact rock and the weak plane, the indexes  $\gamma_i$  and  $\gamma_w$  are introduced.

$$\gamma_i = \frac{3}{2\sqrt{2}} \frac{\tau_{oct}}{S_{oi} \cos \phi_i + \sigma_m \sin \phi_i}, \quad (13)$$

$$\gamma_w = \frac{\tau_w}{S_{ow} \cos \phi_w + \sigma_w \sin \phi_w}. \quad (14)$$

They are used to characterize the shear failure levels of intact rock and weak plane, respectively.

Given the drilling fluid density, calculate the index indexes  $\gamma_i$  and  $\gamma_w$ , and the shear failure of shale causes well-

bore instability when  $\gamma_i > 1$  or  $\gamma_w > 1$ . The maximum value of the two,  $\gamma_{reasonable}$ , is used to judge and analyze the wellbore instability of anisotropy formation.

$$\gamma_{reasonable} = \max(\gamma_i, \gamma_w). \quad (15)$$

The wellbore stability of the anisotropy formation was analyzed based on the strength of the intact rock, the strength of the weak plane, and the overall strength, respectively. And in order to make the results representative, two sets of formation dip angle and inclination azimuth angle parameters were used to calculate the results, respectively, as shown in Figure 7.

As shown in Figures 7(a), 7(c), and 7(e), when the formation dip angle is  $30^\circ$  and the inclination azimuth angle of horizontal well is  $0^\circ$ , the drilling fluid density of  $1.0 \text{ g/cm}^3$  is safe enough. When only considering the weak plane, the safe drilling fluid density needs to reach  $1.5 \text{ g/cm}^3$ . Considering the overall strength of the shale reservoir, the safe drilling fluid density is  $1.5 \text{ g/cm}^3$  under this condition. That is, for shale reservoirs containing weak plane, considering the safety factor



of any angle around the well, the wellbore stability and the safe drilling are determined by the strength of the weak plane. For the situation with a stratum dip angle of 20° and horizontal drilling along an azimuth angle of 45°, as shown in Figures 7(b), 7(d), and 7(f), the overall safe drilling density is 0.9 g/cm<sup>3</sup>, which is also determined by the strength of the weak plane.

During the analysis of wellbore stability of the anisotropy shale reservoir, considering the strength of the weak plane, the lower limit of the safe drilling fluid density window has been greatly increased. The strength weakening of the bedding structure is the reason for the instability of the reservoir shale wellbore.

## 5. Analysis of Wellbore Stability of Reservoir Shale Hydration

Reservoir shale bedding develops well, and the water absorption of bedding and microcrack will further reduce the strength of the weak plane structure, resulting in the instability risk of wellbore. On the other hand, the directional characteristics of the water absorption of the reservoir shale will change the elastic anisotropy of the reservoir shale. Elastic modulus decreases because of the water absorption of reservoir shale. The difference about water absorption amount and speed in parallel and vertical bedding directions will lead to different degrees of the reduction in elastic modulus in each direction, thereby changing the anisotropy degree of elastic parameters.

By calculating the wellbore stress under different elastic modulus ratios, the influence of reservoir shale water absorption direction differences on the wellbore stability is explored. The elastic modulus ratio  $n$  is defined as the ratio of the elastic modulus vertical to the bedding plane, to those in the plane of isotropy, that is

$$n = \frac{E'}{E}. \quad (16)$$

Keep the elastic modulus in the bedding plane unchanged, then change the normal elastic modulus of the bedding plane, make the  $n$  value equal to 1, 0.75, 0.5, and 0.25 in turn, and calculate the maximum principal stress of the wellbore. The results are shown in Figure 8.

As the inclination angle increases from 0° to 90°, the influence of elastic modulus ratio on the principal stress distribution of wellbore increases gradually. The elastic modulus ratio hardly affects the wellbore stress distribution in straight wells and small-deviated wells. In horizontal wells, the elastic modulus ratio changes both the magnitude and angle of wellbore stress distribution. When analyzing of wellbore stability of horizontal wells in reservoir shale, the change of anisotropy caused by shale water absorption should not be ignored.

## 6. Summary and Conclusions

- (1) Combined with the reservoir shale in the Fuling shale gas field, the sensitive clay mineral content,

Zeta potential, cation exchange capacity (CEC), specific surface area, roller recovery, capillary absorption time (CST), and water absorption expansion tests show that the swelling of shale in Wufeng-Longmaxi formation is not strong, hydration dispersion is weak, expansion and dispersion are not the main reason for the wellbore instability, and conventional hydration expansion and dispersion parameters cannot characterize shale gas reservoirs well

- (2) Bedding and microcracks of reservoir shale in Wufeng-Longmaxi formation develop highly, and its rock mechanical characteristics have the macroscopic and microscopic strength and elastic anisotropy. At the same time, the initial water saturation of the shale reservoir is low, and the spontaneous imbibition ability of the shale gas reservoir is strong. Elasticity and strength anisotropy under imbibition conditions are the important parameters of wellbore stability evaluation
- (3) High stress is the root cause of wellbore instability of the shale reservoirs, and weak plane strength increases the risk of wellbore instability. Bedding and microcracks have an important impact on reservoir fluid absorption and wellbore stability. Bedding provides a channel for rapid imbibition and increases the imbibition volume. Reservoir fluid absorption causes cracks propagation and strength weakening, resulting in wellbore instability
- (4) In the analysis of wellbore stability considering the interaction between fluid and shale, it should be paid attention to the changes in strength and elastic anisotropy caused by water absorption of the reservoir shale. The key to maintaining wellbore stability in shale gas reservoirs is to achieve multilevel effective plugging of bedding, microcracks, and macropores

## Data Availability

All data are available on request.

## Conflicts of Interest

The authors declare that they have no conflicts of interest.

## Acknowledgments

The research is supported by Scientific Research and Technology Development Project of CNPC (Numbers 2020F-50 and 2021DJ7401) and Scientific Research and Technology Development Project of PetroChina Company Limited (Number 2022KT1603).

## References

- [1] H. Wang, Y. Liu, D. Dong, Q. Zhao, and D. Du, "Scientific issues on effective development of marine shale gas in southern China," *Petroleum Exploration and Development*, vol. 40, no. 5, pp. 615–620, 2013.

- [2] O. Gaede, F. Karpfinger, J. Jocker, and R. Prioul, "Comparison between analytical and 3D finite element solutions for borehole stresses in anisotropic elastic rock," *International Journal of Rock Mechanics and Mining Sciences*, vol. 51, pp. 53–63, 2012.
- [3] J. Zhang, "Borehole stability analysis accounting for anisotropies in drilling to weak bedding planes," *International Journal of Rock Mechanics and Mining Sciences*, vol. 60, pp. 160–170, 2013.
- [4] L. Liang, J. Xiong, and X. Liu, "Experimental study on crack propagation in shale formations considering hydration and wettability," *Journal of Natural Gas Science and Engineering*, vol. 23, pp. 492–499, 2015.
- [5] B. Wu, X. Zhang, R. G. Jeffrey, and K. Mills, "Analytical solutions for an extended overcore stress measurement method based on a thermo-poro-elastic analysis," *International Journal of Rock Mechanics and Mining Sciences*, vol. 89, pp. 75–93, 2016.
- [6] H. Singh, "A critical review of water uptake by shales," *Journal of Natural Gas Science and Engineering*, vol. 34, pp. 751–766, 2016.
- [7] D. Liu, H. Ge, Y. Shen, H. Liu, and Y. Zhang, "Experimental investigation on imbibition characteristics of shale with highly developed bedding fractures," *Journal of Natural Gas Science and Engineering*, vol. 96, article 104244, 2021.
- [8] C. Fang, Z. Huang, Q. Wang, D. Zheng, and H. Liu, "Cause and significance of the ultra-low water saturation in gas-enriched shale reservoir," *Natural Gas Geoscience*, vol. 25, no. 3, pp. 471–476, 2014.
- [9] C. Fang, Z. Huang, Q. Wang, L. You, Y. Kang, and Y. Wang, "Simulation of ultra-low water saturation in shale gas reservoirs and its significance," *Geochimica*, vol. 44, no. 3, pp. 267–274, 2015.
- [10] H. Liu and H. Wang, "Ultra-low water saturation characteristics and the identification of over pressured play fairways of marine shales in South China," *Natural Gas Industry*, vol. 33, no. 7, pp. 140–144, 2013.
- [11] Y. Kang, J. She, C. Lin, and Y. Lijun, "Brittleness weakening mechanisms of shale soaked by drilling & completion fluid," *Chinese Journal of Theoretical and Applied Mechanics*, vol. 48, no. 3, pp. 730–738, 2016.
- [12] B. Amadei, *Rock Anisotropy and the Theory of Stress Measurements*, Springer-Verlag, Berlin, 1983.
- [13] B. S. Aadnoy, *Continuum Mechanics Analysis of the Stability of Inclined Boreholes in Anisotropic Rock Formations*, [Ph.D. thesis], Norwegian Institute of Technology, Trondheim, 1987.
- [14] D. J. Gupta and M. Zaman, "Stability of boreholes in a geologic medium including the effects of anisotropy," *Applied Mathematics and Mechanics*, vol. 20, no. 8, pp. 837–866, 1999.
- [15] L. Chang, *Study on Mechanics Problems of Borehole Stability in Anisotropic Formation*, China University of Petroleum, 2015.
- [16] C. Mian, J. Yan, and Z. Guangqing, *Petroleum Related Rock Mechanics*, Science Press, Beijing, 2008.
- [17] A. M. Al-Ajmi and R. W. Zimmerman, "Relation between the Mogi and the Coulomb failure criteria," *International Journal of Rock Mechanics and Mining Sciences*, vol. 42, no. 3, pp. 431–439, 2005.
- [18] Z. Wang and J. Sun, *Practice and Understanding of Experimental Well Group Development in Fuling Shale Gas Field*, vol. 188-189, China Petrochemical Press, Beijing, 2014.
- [19] J. Gao, J. Deng, K. Lan, Z. Song, Y. Feng, and L. Chang, "A poro-thermoelastic solution for the inclined borehole in a transversely isotropic medium subjected to thermal osmosis and thermal filtration effects," *Geothermics*, vol. 67, pp. 114–134, 2017.